Journal of Alloys and Compounds 480 (2009) 157–160

Contents lists available at ScienceDirect

Journal of Alloys and Compounds

journal homepage: www.elsevier.com/locate/jallcom

Iron containing 3d–4f compounds: Effect of alternative processing on local interactions and storage properties

G. Filoti[a,*], P. Palade[a], D. Lupu[b], F. Stromberg[c], G. Schinteie[a], O. Ardelean[b], V. Kuncser[a]

[a] National Institute for Materials Physics, Atomistilor Street 105bis, 077125 Bucharest-Magurele, Romania
[b] National Institute for Isotopic and Molecular Technologies, Donath street 71, 400293 Cluj-Napoca, Romania
[c] University Duisburg-Essen, Lothar Street 1, 47048 Duisburg, Germany

ARTICLE INFO

Article history:
Received 15 July 2008
Received in revised form 5 October 2008
Accepted 6 October 2008
Available online 22 November 2008

PACS:
75.50.Cc
82.80.Ej
63.70.+h
81.90.+c

Keywords:
$LaNi_{5-x}Fe_x$
Magnetic properties
Mössbauer
Debye temperature
Hydrogen storage

ABSTRACT

Samples of $LaNi_{5-x}Fe_x$ were prepared by arc melting and subsequent melt spinning procedure. Structural, magnetic and Mössbauer investigations were performed for physical characterization while the hydrogen storage properties were carefully analyzed. Detailed discussions concerning the sample's quality, the site assignment, the effect of temperature and applied fields on hyperfine parameters and the related Debye temperatures were provided.

1. Introduction

The $LaNi_5$ is one famous member of the series of 3d–4f compounds, mainly due to high hydrogen storage capacity and its use in Ni-metal hydride rechargeable batteries [1]. It was reported [2] that the substitution of Ni with Fe up to 1.2 atoms conserves the initial $CuCa_5$ type hexagonal structure. It is established [3,4] that iron substitution in the $LaNi_5$ lattice increases the hydrogen storage and cycling performances. The structure accommodates Ni atoms in two positions, labelled "2c" and "3g".

In the Fe substituted compound, the iron occupies both Ni positions, in a ratio depending on the amount of substitution, as well as on preparation procedure and subsequent processing [5]. In our attempt to improve the hydrogen storage properties, after producing the ingots using arc melting, a part of the sample was rapidly quenched purged via melt spinning procedure. In the following, there are discussed the structural, magnetic and, finally, the hydrogen sorption/de-sorption data, mostly on samples obtained by rapid quenching, in regard to the arc melting "as prepared" ones.

2. Experimental

The arc melting was realized using a home made device containing an electrolytic Cu bath and a 3 mm Tungsten electrode, all placed in a very pure Ar atmosphere over-passing with 0.1 bars the normal pressure. The melt spinning was a Buehler type with electrolytic copper wheel (20 cm diameter) rotating with a speed of ~25.2 m/s. An over-pressure of 0.4 bars was assured inside the chamber. The purging hole in the quartz tube nozzle had a 0.5 mm diameter.

The crystal structure of all prepared samples was identified by X-ray diffraction on a Bruker-AXS D8-Advance series spectrometer using the ICDD database. The diffractometer was set in a parallel monochromatic configuration for the incident beam asymmetric channel-cut (ACC) monochromator.

The magnetic ac susceptibility was measured on a MPMS SQUID magnetometer (Quantum Design) with ac option. The actual measurements were done at an excitation frequency of 10 Hz and amplitude of 4 Oe. The magnetization versus field, $M(H)$ curves, was performed at 1.8 K and fields up to 5 T.

The Mössbauer spectra (MS) were acquired using a constant acceleration spectrometer with symmetrical waveform. The isomer shifts are referred to bcc Fe at room temperature. A Helium bath cryostat was used for temperature dependent Mössbauer measurements and those in applied field (up to 5 T).

All the kinetics curves and pressure-composition isotherms have been measured at 20 °C using a home made Sievert (volumetric) apparatus. Prior to hydrogenation, the samples were degassed under vacuum at 300 °C for 1 h. After temperature sta-

---

[*] Corresponding author. Tel.: +40 213690170; fax: +40 213690177.
E-mail address: filoti@infim.ro (G. Filoti).

0925-8388/$ – see front matter © 2008 Elsevier B.V. All rights reserved.
doi:10.1016/j.jallcom.2008.10.008

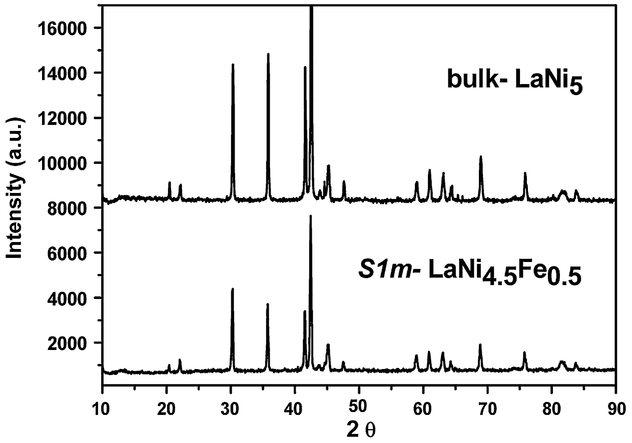

Fig. 1. X-ray diffraction spectra of substituted and non substituted samples.

bilization in the instrument's reservoir, the hydrogen was purged in the sample compartment. The H_2 absorption was measured by pressure changing in calibrated volumes. The absorption was performed under almost constant hydrogen pressure of 6 atm. The de-sorption kinetics curves were obtained under low H_2 pressures (about 0.2 atm).

3. Results and discussion

After careful weight (considering some loss of La) of elemental materials, two samples of $LaNi_{5-x}Fe_x$ with $x = 0.5$ (sample code *S1*) and $x = 0.25$ (*S2*) were prepared by arc melting. Half of the amount was subsequently processed via melt spinning method giving rise to samples labelled *S1m* and, respectively *S2m*. The X-ray diffraction, of new prepared samples, confirms the $CaCu_5$ hexagonal structure type of substituted $LaNi_5$ under above mentioned procedures, as observed via the plots of the Fig. 1.

The Fe is homogeneous distributed inside of the cell structure giving rise to well defined single phase as exemplified by above structural data, but also by data of the ac susceptibility measurements for sample *S1m* (Fig. 2). Both χ' (in phase) and χ'' (out of phase) susceptibility showed a pronounced maximum, revealing a ferromagnetic type interaction and granting a Curie temperature (T_C) of 14.6 K from χ' plot. Measurements at other frequencies, than the 10 Hz shown one, evidenced the same temperature value of the maximum, leaving out a possible clustering process of the iron atoms. The previously reported compounds, having the same or rather close composition, show a T_C close to 40 K for $x = 0.4$ [6], then ~50 K from Mössbauer [7] and, respectively, ~75 K from dc magnetic measurements [7], or 50 ± 5 K, again for $x = 0.4$ [9]. The low temperature values of T_C of the sample *S1m* are also pointing to a homogeneous distribution of Fe substitution on both "3g" and "2c" sites. The magnetization data for sample *S1m*, in fields up to 50 T, at 1.8 K (Fig. 3) exhibits a tendency to saturation at 1 μ_B value, far from the 2.5 μ_B theoretical evaluations [8] made for $LaNi_{5-x}Fe_x$ system. Subsequently, we will report the Mössbauer data on the two melt spun samples only.

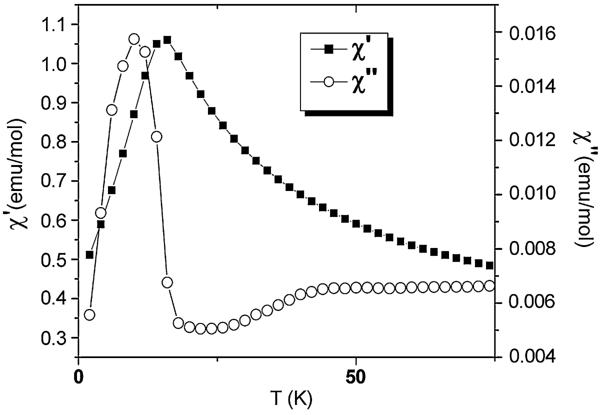

Fig. 2. The ac susceptibilities (χ'—in phase and χ''—out of phase) of the sample *S1m*.

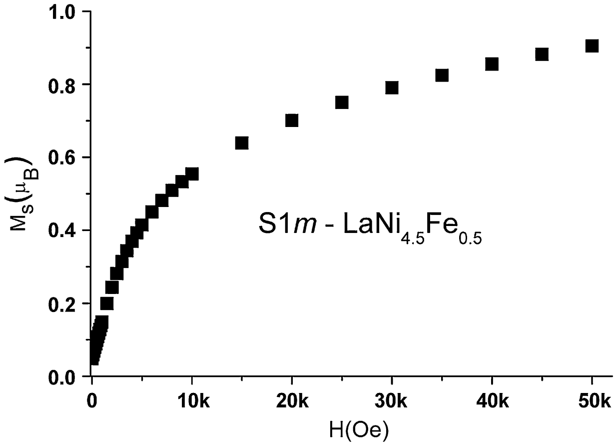

Fig. 3. Magnetization plot of *S1m* melt spun sample at 1.8 K.

The Mössbauer data unambiguously show that iron substitutes Ni on both of its crystallographic sites. Two well defined patterns appeared, for example, at 4.2 K (sextets) or at 300 K (doublets). In the Fig. 4 the spectra of sample *S1m* are displayed (from bottom-up) either at 4.2 K (with and without applied field), at higher temperatures (80 and 300 K) and finally, after the hydrogen up-taking (the upper one). The Mössbauer spectra of sample *S2m* confirmed similar type of interactions and the same behaviour as *S1m*, as provided by the tables, which contain the values of the field at nucleus (B), the isomers shift (IS) and quadrupole splitting (QS), as well as the relative area of each pattern for the sextets at 4 K (Table 1) and for doublets at other temperatures (Table 2).

The two sextets, 4.2 K, are characterised by internal fields (blocked spin configuration) of 19.5(4) T and, respectively 17.2(4) T. The mentioned values could be compared with the 17.7 to 22.7 T range of previous data [7,9,11] fitted considering either unique sextet or hyperfine field distributions. The measurements in applied field of 5 T confirmed the ferromagnetic behaviour, already mentioned from magnetic measurements, both sextets showing reduced splittings (fields of 18.4 and 15.2 T).

For the doublets of the sample *S1m* the IS of one is negative (−0.14 mm/s at 300 K and −0.06 mm/s at 80 K) and of the second is positive (+0.18 mm/s at 300 K and, respectively, 0.26 mm/s at 80 K). The spectra, at 300 K, provided QS of 0.96 mm/s and, respectively, 0.56 mm/s for the same sequence of doublets and larger values at 80 K (Table 2). The *S2m* provided similar IS and QS values, but with other populations per sites (Table 2). These values and those for hydrogenated sample are inside of a large range of earlier reported data [5,7,9–11].

Table 1
Relevant Mössbauer parameters of the sextets appeared at 4 K, without and with applied field.

Sample	B_1 (T)	B_2 (T)	IS_1 (mm/s)	IS_2 (mm/s)	A_1 (%)	A_2 (%)
S1m	19.5(4)	17.2(4)	0.19(3)	0.22(3)	69.4	30.6
S1m + 5T	18.2(4)	15.2(4)	0.11(3)	0.12(3)	68.7	31.3
S2m	17.2(4)	13.3(4)	0.18(3)	0.21(3)	64.9	35.1

Table 2
Parameters of Mössbauer doublets at different temperatures, including the hydrogenated sample.

Sample	T (K)	QS_1 (mm/s)	QS_2 (mm/s)	IS_1 (mm/s)	IS_2 (mm/s)	A_1 (%)	A_2 (%)
S1m	80	1.02	0.62	−0.06	+0.26	75.4	24.6
	300	0.96	0.56	−0.14	+0.18	91.3	8.7
S2m	80	1.08	0.58	−0.08	+0.27	80.5	19.5
	300	0.98	0.53	−0.12	+0.22	95.5	4.5
S1m + H	300	1.12	0.93	−0.10	+0.21	80.2	19.8

Errors: ±0.03 mm/s.

The IS and QS are very sensible to local coordination such as the surrounding configuration, number of neighbours, distances to closest neighbours (first coordination sphere) and their elemental type via atomic or ionic radius. The central atom for "c" coordination is surrounded by 6 Ni in "3g" at 0.246 nm and at larger distances by 3 Ni in "2c" at 0.290 nm and 3 La in "1a" at 0.290 nm. The closest 6 Ni neighbours form a double pyramid with triangular base, sharing the same apex. The "g" configuration has 4 Ni on 2c at 0.246 nm and other 4 Ni in "3g" at 0.250 nm and rather at far distance 4 La in "1a" at 0.320 nm. The first 8 Ni, at rather close distances, are arranged in a double pyramid adjoined by central atom both with square base. The strongly influencing the Mössbauer parameters are the closest surroundings, forming double pyramids with triangular ("2c" site) and, respectively, square ("3g" site) base, as above described.

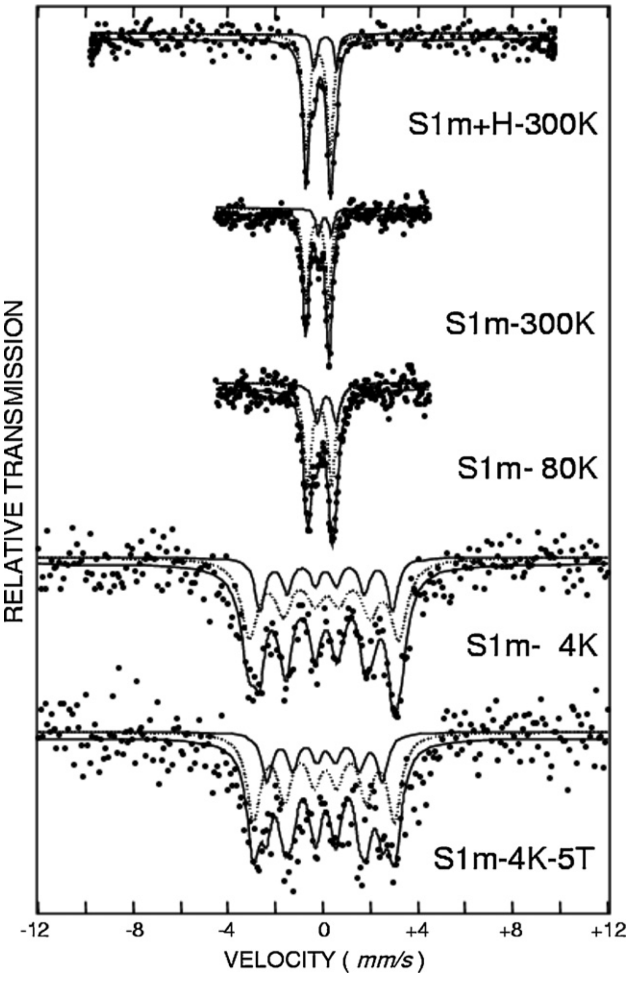

Fig. 4. Mössbauer spectra of sample *S1m* at different conditions.

The assignment of the Mössbauer patterns was performed taking into account various considerations: such as the occupancy ratio of the two crystallographic sites, mostly often used, but also another approach of considering the local configuration. There is a more numerous atoms surrounding and larger charge asymmetry for position "3g". Therefore the doublet with larger QS and relative area and with negative IS has to belong to the "3g".

Band structure calculations were performed using *Wien2k* code [12]. We built 2 × 1 × 1 supercells in which one "2c" respectively "3g" Ni atom was replaced by one Fe atom in order to simulate the Ni substitutions by Fe in the $LaNi_5$ unit cell according to $LaNi_{4.5}Fe_{0.5}$ formula. *Wien2k* code uses the full-potential linear augmented + local orbitals method (LAPW + LO), a very precise approach for calculating electronic properties for crystals, even it is consuming more time than pseudopotential methods. Muffin-tin radii of 2.50 a.u. for La respectively 2.08 a.u. for Ni and Fe have been used in order to avoid overlapping between muffin tin spheres during geometry optimization steps. The exchange-correlation energy was calculated using LSDA (local spin density approximation) and the Fermi energy was obtained by the modified tetrahedron method. About 100 plane waves per atom were used to expand the one-electron wave functions in the interstitial region while inside muffin-tin spheres an expansion up to an orbital quantum number of $l = 12$ was used. The charge density and the potential inside the muffin tin spheres were expanded into lattice harmonics up to $L = 6$ for all atoms. A k-mesh with 390 points in the irreducible wedge of the first Brillouin zone was used. The electric field gradients, main factor of QS, and the magnetic hyperfine fields to iron nuclei were computed using the charge density inside the unit cell. The calculations take into account not only the modification of the valence charge but also core charge modification due to crystal potential with very important contribution to the hyperfine parameters values. First principles band structure calculations allowed also the estimation of the electron density to nucleus $\rho(0)$ what is linearly related to IS.

The theoretical results provided a QS value of 1.15 mm/s for Fe substituting Ni at "3g" site and 0.80 mm/s for Fe at "2c" site, slightly larger than the experimental ones. The ratio of the QS values for the two sites (QS(Fe-3 g)/QS(Fe-2c)) obtained from calculations is 1.44, close to the same ratio obtained at 80 K for the experimental values, of 1.64 value. The calculated density to nucleus, $\rho(0)$, for the Fe "3g" atom is noticeable higher than one for the Fe "2c", in agreement with the experimental IS trend. Lower calculated values were obtained for magnetic hyperfine fields (14.2 T for Fe-"3g" and 9.7 T for Fe "2c") compared to the experimental ones (19.5 T and respectively 17.2 T). The difficulty to describe correctly the magnetic properties of the strongly correlated systems by a proper exchange-correlation function could explain the differences obtained for the magnetic hyperfine fields, between the theoretical and experimental values.

The calculations undoubtedly confirmed that the doublet with higher QS and B and, respectively, more negative IS should be assigned to the "3g" atom.

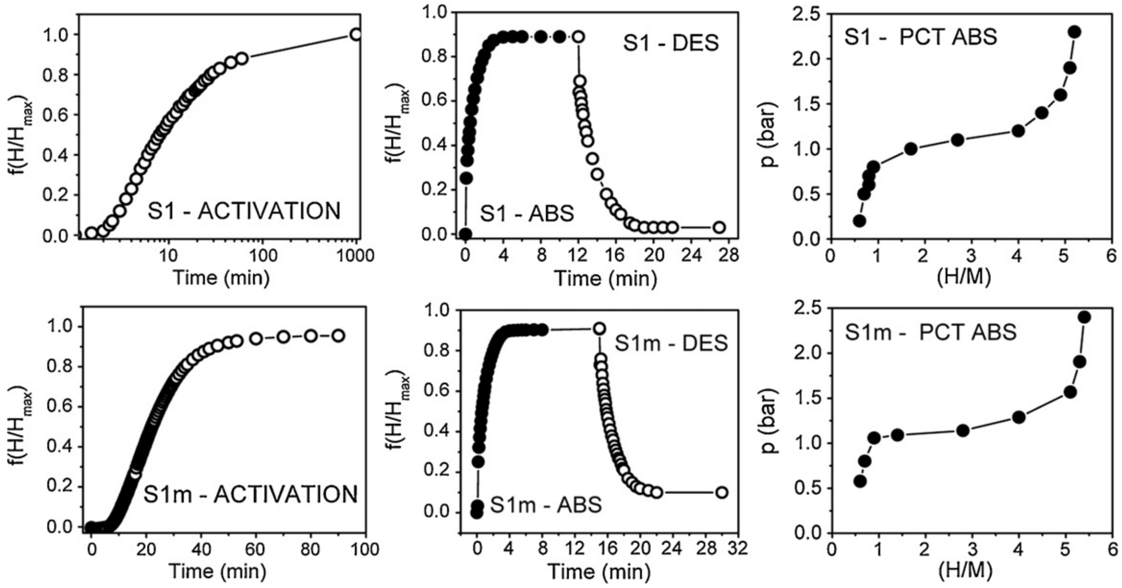

Fig. 5. Activation, absorption/de-sorption kinetics and PCT curves for bulk and melt spun $LaNi_{4.5}Fe_{0.5}$.

The observed change of relative area of the two patterns with temperature has a bearing on different Debye temperatures (θ_D) of each site. The spectral area is proportional with the Lamb–Mössbauer factor, being expressed for temperatures higher than θ_D as: $f_{\mathrm{LM}} = \exp(-E_R/h\omega_D) = \exp(-6E_R T/k\theta_D^2)$. The θ_D can be obtained by plotting the natural logarithm of absolute area of each pattern versus *T*. Noticeable different and rather low Debye temperatures have resulted for each site: 152(2) K for "3g" and 134(2) K for "2c", supporting the observed modification of relative areas, especially at higher temperatures, as evidenced by data from Table 2.

The activation of the sample *S1* completes in about 1000 min while for the sample *S1m* in about 100 min as shown in Fig. 5, proving the importance of the melt-spinning technique for obtaining hydrogen storage materials with improved properties. After few cycles, *S1m* exhibits similar absorption kinetics compared to *S1* (absorption completes in 3 min for both samples) but slightly better de-sorption kinetics than *S1* (Fig. 5). The improved desorption and the easier activation for the melt spun sample may be explained by more homogenous Fe distribution and finer grain morphology with catalytic effect. The PCT curves show almost the same middle plateau pressure of about 1.15 bar for both samples.

4. Conclusion

The new samples of $LaNi_{5-x}Fe_x$ compounds, prepared via melt spinning procedure, showed improved hydrogen storage properties. The more homogenous Fe distribution, gave rise to lower ordering temperature of the ferromagnetic state and improved storage properties. The assignment of Fe patterns was performed taking into account distinct specific close surroundings, their population and values provided by DFT calculation of the Mössbauer parameters. The low values of Debye temperatures per site support the behaviour of related Mössbauer parameters.

Acknowledgements

This work was financially supported via the research project 707/2006 by "MENER" Romanian National program. We deeply acknowledge the help of Prof. Dr. Heiko Wende for "in field" measurements and presentation suggestions as well as the one of Dr. Yanhua Lan for magnetic measurements.

References

[1] P.H.L. Notten, R.E.F. Einerhand, J.L.C. Daams, J. Alloys Compd. 210 (1994) 221–232.
[2] M. Escorne, J. Lamloumi, A. Percheron-Guegan, J.C. Achard, A. Mauger, J. Magn. Magn. Mater. 65 (1987) 63–70.
[3] S. Vivet, M. Latroche, Y. Chabre, J.-M. Joubert, B. Knosp, A. Percheron-Guégan, Phys. B 362 (2005) 199–207.
[4] H. Dhaou, F. Askri, M. Ben Salah, A. Jemni, S. Ben Nasrallah, J. Lamloumi, Int. J. Hydrogen Energy 32 (2007) 576–587.
[5] S.J. Campbell, R.K. Day, J.B. Dunlop, A.M. Stewart, J. Magn. Magn. Mater. 31–34 (1983) 167–168.
[6] M. Escomel, A. Maugerz, J. Lamloumi, A. Percheron-Guégan, Solid State Commun. 89 (1994) 761–765.
[7] J. Lamloumi, A. Percheron-Guégan, J.A. Achard, G. Jehanno, D. Givord, J. Phys. 45 (1984) 1643–1652.
[8] J.B. Yang, C.Y. Tai, G.K. Marasinghe, G.D. Waddill, O.A. Pringle, W.J. James, Y. Kong, Phys. Rev. B 63 (2000) 1–7, 014407.
[9] M. Escorne, J. Lamloumi, A. Percheron-Guégan, J.A. Achard, A. Mauger, G. Jehanno, J. Appl. Phys. 63 (1988) 4121–4123.
[10] C.Y. Tai, C. Tan, G.K. Marasinghe, O.A. Pringle, W.J. James, M. Chen, W.B. Yelon, J. Gebhardt, N. Ali, IEEE Trans. Magn. 35 (1999) 3346–3348.
[11] D. Niarchos, P.J. Viccaro, G.K. Shenoy, B.D. Dunlap, A.T. Aldred, Hyp. Int. 9 (1981) 563–570.
[12] P. Blaha, K. Schwarz, G. Madsen, D. Kvasnicka and J. Luitz, *WIEN2k*, An Augmented Plane Wave + Local Orbitals Program for Calculating Crystal Properties (Karlheinz Schwarz, Tech. Universität Wien, Austria), 2001. ISBN 3-9501031-1-2.